ARTICLE

A Mutation in *HOXA2* Is Responsible for Autosomal-Recessive Microtia in an Iranian Family

Fatemeh Alasti,[1,2] Abdorrahim Sadeghi,[2,3,8] Mohammad Hossein Sanati,[4] Mohammad Farhadi,[5] Elliot Stollar,[6] Thomas Somers,[7] and Guy Van Camp[1,*]

Microtia, a congenital deformity manifesting as an abnormally shaped or absent external ear, occurs in one out of 8,000–10,000 births. We ascertained a consanguineous Iranian family segregating with autosomal-recessive bilateral microtia, mixed symmetrical severe to profound hearing impairment, and partial cleft palate. Genome-wide linkage analysis localized the responsible gene to chromosome 7p14.3-p15.3 with a maximum multi-point LOD score of 4.17. In this region, homeobox genes from the *HOXA* cluster were the most interesting candidates. Subsequent DNA sequence analysis of the *HOXA1* and *HOXA2* homeobox genes from the candidate region identified an interesting *HOXA2* homeodomain variant: a change in a highly conserved amino acid (p.Q186K). The variant was not found in 231 Iranian and 109 Belgian control samples. The critical contribution of HoxA2 for auditory-system development has already been shown in mouse models. We built a homology model to predict the effect of this mutation on the structure and DNA-binding activity of the homeodomain by using the program Modeler 8v2. In the model of the mutant homeodomain, the position of the mutant lysine side chain is consistently farther away from a nearby phosphate group; this altered position results in the loss of a hydrogen bond and affects the DNA-binding activity.

Introduction

Microtia (MIM %600674) is a congenital deformity of the outer ear and occurs in approximately one in 8,000–10,000 births. It is characterized by a small, abnormally shaped outer ear. It can be unilateral or bilateral. Almost 80% of the microtic cases are unilateral. In unilateral microtia, the right ear is more frequently affected (approximately 60% of the unilateral cases).[1–3] The patients with unilateral microtia usually have normal hearing in the other ear. Microtia occurs more commonly in males. Microtia and aural atresia MIM (%607842), referring to the narrowing or absence of the ear canal, tend to occur together because the outer ear and the middle ear evolve from a common embryological origin.[1–5]

Microtia is divided into four grades. Although most of the features of a normal ear, such as the lobule, helix, and anti-helix, are present in grade I, the external ear is smaller than normal. This can occur with or without aural atresia. In grade II, the normal features of the external ear are absent. A lobule, a helix, and an anti-helix are present, but they are small and not well formed. In grade III, the external ear consists of a vertical skin appendage with a malformed lower end of the ear lobe. There is usually firm tissue made up of cartilaginous vestige at the upper end. The extreme case when there is no external ear or auditory canal is called anotia, or microtia grade IV.[6]

Syndromic forms of microtia occur in conjunction with other abnormalities. The associated malformations are mainly found in the bilateral cases. The most common associated malformations are cleft lip or palate, limb-reduction defects, renal abnormalities, cardiac defects, anophtalmia or microphtalmia, polydactyly, and vertebral anomalies, which are combined with hearing loss.[2,3,7]

The most common syndromes associated with microtia are hemifacial microsomia, also known as Goldenhar radial defect syndrome (HFM [MIM %164210]), and Treacher Collins syndrome (TCS [MIM #154500]). There are other syndromes, such as Nager syndrome (MIM 154400), CHARGE association[1,3,8] (MIM #214800), and Facio- or Oculo-auriculo-vertebral spectrum (OAV [MIM %164210]), which involves facial, renal, vertebral, and eyelid defects. Goldenhar syndrome is part of the OAV spectrum.[9,10]

The auricle results from the fusion of six auricular hillocks from the first and second branchial arches that surround the first pharyngeal groove during the sixth week of gestation. The auricle is usually complete by the 12th week. Initially, the auricle forms at the base of the neck, but as the mandible develops, the auricles migrate to their normal anatomical position.[11] Microtia occurs when the tissues that form the auricle fail to develop properly.

Although the causes of microtia are poorly understood, gestosis, anemia, and certain medications, such as isotretinoin or thalidomide, taken by the mother during pregnancy have been implicated.[4,12] However, it is believed that genetic components are also involved because additional familial cases are found in 9%–34% of microtic

[1]Department of Medical Genetics, University of Antwerp, 2610 Antwerp, Belgium; [2]Department of Molecular Genetics, National Institute for Genetic Engineering and Biotechnology, Tehran, Iran; [3]Department of biology, the faculty of sciences, Tarbiat modarres University, Tehran, Iran; [4]Department of Medical Genetics, National Institute for Genetic Engineering and Biotechnology, Tehran, Iran; [5]Iran Cochlear Implant Center, Rassoul-e Akram Hospital, Iran University of Medical Sciences, Tehran, Iran; [6]Hospital for Sick Children, Department of Molecular Structure and Function, Toronto, Ontario, Canada; [7]University Department of Otolaryngology, St. Augustinus Hospital, University of Antwerp, Antwerp, Belgium
[8]Present address: Faculty of Medicine, The Arak University of Medical Sciences, Arak, Iran.
*Correspondence: guy.vancamp@ua.ac.be
DOI 10.1016/j.ajhg.2008.02.015.

patients.[10,13] Monogenic forms with autosomal-dominant or -recessive inheritance of microtia,[10,14–17] as well as chromosomal abnormalities[1,3] including four trisomies (13, 18, 21, and 22) and three deletions of a chromosome arm (5p−, 18p−, and 18q−), have been reported.[3,18]

We report on a missense mutation in the *HOXA2* (MIM *604685) homeobox gene in a consanguineous family with bilateral microtia, severe to profound hearing impairment, and partial cleft palate. This is the first report of a mutation in this gene in a human Mendelian disorder.

Methods and Materials

Subjects

We ascertained a consanguineous Iranian family IR-SA-27 from Persian ethnicity and segregating with autosomal-recessive bilateral microtia. This family contains four affected individuals. Blood samples were taken from ten family members. DNA samples of 231 unrelated Iranian and 109 Belgian nonmicrotic hearing individuals were used as controls. All of the participating individuals from the family IR-SA-27 signed an informed consent form prior to their inclusion in this study. This research was approved by the Institutional research council at the National Institute for Genetic Engineering and Biotechnology (NIGEB), Tehran, Iran and the Ethical Committee of the University of Antwerp, Belgium.

Clinical Examinations

Otoscopy

Three affected members of the family IR-SA-27 were examined by an otorhinolaryngologist in the Rasoul-e-Akram hospital in Tehran, Iran. These affected individuals underwent otoscopic examinations for outer- and middle-ear morphology. Patients were physically examined and interviewed so that they could be evaluated for syndromic features including lip or palate cleft, limb defects and renal, cardiac, eye, neurological and mental abnormalities.

Auditory and Tympanotomy Tests

Pure tone audiometry was carried out under quiet ambient conditions at frequencies ranging from 250 to 8000 Hz for air conduction and 250 to 4000 Hz for bone conduction. The audiometric testing was performed according to standard protocols.

Vestibular Examinations

For evaluation of the vestibular system, videonystagmography (VNG), including spontaneous nystagmus, evaluation of saccade, gaze, and rebound nystagmus, positional tracking, and hallpike examinations as well as bithermal caloric testing, was performed.

High-Resolution Computer Tomography Scan and Magnetic Resonance Imaging

For tracing inner-ear malformations and assessing the ossicular mass, the nature of the atretic plate (either bony or soft), the position and course of the facial nerve, the degree of development of the external ear canal, and the degree of mastoid pneumatization, high-resolution computer tomography (CT) and magnetic resonance imaging (MRI) scans were carried out. An axial and coronal high-resolution CT scan (1 mm slices in coronal and transverse directions) of the temporal bone was performed for individuals with microtia and hearing impairment. Two patients underwent MRI of the ears. Sagittal and axial T1, FSE T2, and FLAIR in addition to coronal T2-W sequences were obtained. The patient with a facial motor problem underwent an additional brain MRI. Sagittal T2 and axial T1, FSE T2, and FLAIR, in addition to post-contrast axial, coronal, and sagittal T1-weighed sequences, were obtained for the brain MRI.

Additional Clinical Tests

Blood biochemistry, urine analysis, cell blood counting (CBC), electrocardiography, and radiological X-ray examinations were also performed. Blood sugar, urea, creatinine, uric acid, cholestrol, triglycerids, calcium, phosphate, sodium, potassium, and alkaline phosphatase were measured for biochemical analysis. Urine was analyzed for color, appearance, specific gravity, pH, the presence of proteins, glucose, ketones, bilirubin, urobilinogen, and the presence of blood cells and bacteria. Radiographs were taken from different bones, including those of the skull, hands, feet, arms, wrists, legs, tibia, cervical spine, pelvis, and chest. Kidneys were investigated bilaterally with ultrasonography.

Genotyping

Genomic DNA was isolated from EDTA-treated peripheral blood samples from ten family members according to a standard salting-out method.[19] Genome-wide linkage analysis was performed with 500 short tandem repeat polymorphic (STRP) markers across all chromosomes by deCode Genetics (Reykjavik, Iceland). For subsequent fine mapping, additional STRP markers in the linked region were genotyped. PCR reactions for STRP markers were performed according to a standard procedure. The analysis of fluorescently labeled amplified STRP markers was carried out by capillary electrophoresis with an ABI 3130 DNA sequencer (XL Genetic Analyzer). Alleles were assigned with GeneMapper v.3.7 (Applied Biosystem).

Linkage Analysis

Two-point parametric linkage analysis was performed with the Superlink version 1.4 option of the easyLINKAGE plus version 4.01beta software, and multipoint LOD scores were calculated with the Simwalk version 2.91 option of easyLINKAGE. This program estimates allele frequencies on the basis of pedigree data. Microtia was assumed to be fully penetrant without phenocopies and to have an autosomal-recessive mode of inheritance. Recombination frequencies were considered to be identical in males and females. The gene frequency for microtia was set at one in 10,000.

DNA Sequencing

The exons of *HOXA1* (MIM *142955) and *HOXA2* genes in the *HOXA* cluster and their splice junctions were PCR amplified with 30 ng genomic DNA, 200 μM dNTPs, and 0.5 μM primers. The quality of the PCR products was verified by electrophoresis on 1.5% agarose gel, and subsequent DNA sequencing was performed on an ABI 3130 automated sequencer (XL Genetic Analyzer) with the big-Dye terminator cycle sequencing kit version 3.1 (Applied Biosystem, USA). The sequence of the primers used for *HOXA1* exon amplification was previously reported.[14] The sequence of the primers for amplifying the exons of *HOXA2* and the annealing temperatures are presented in Table S1 in the Supplemental Data. ConSeq scores were used as a measure of evolutionary conservation of amino acids. These scores vary from 1 (variable) to 9 (conserved).[20] The ConSeq program also suggests whether the residue is buried (b) or exposed (e) and whether it is a functional (f) or a structural residue (s).

Model-Building Process

The Human HOXA2 protein was aligned with the *Drosophila melanogaster* Antennapedia homeodomain, which has 58%

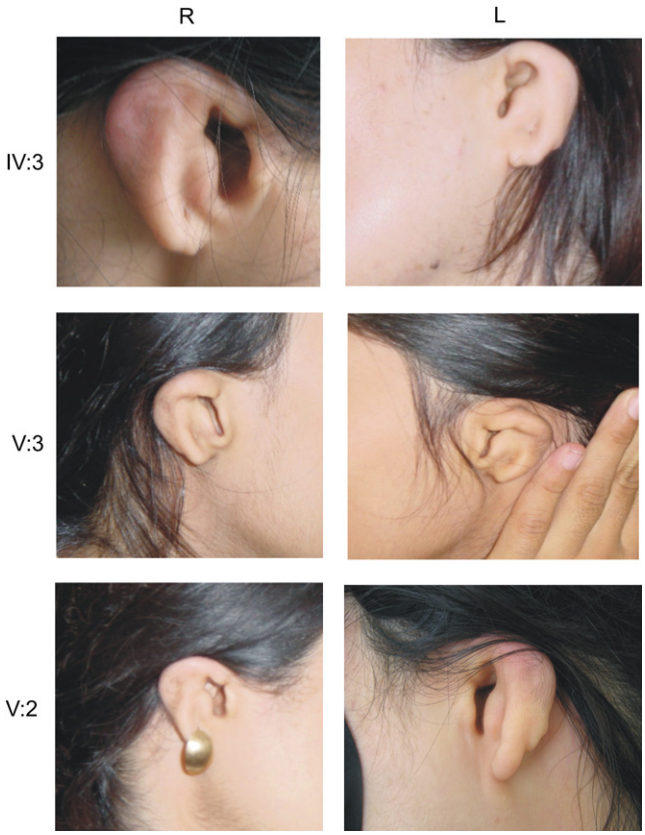

Figure 1. Photographs of the Microtic ears of Three Affected Family Members

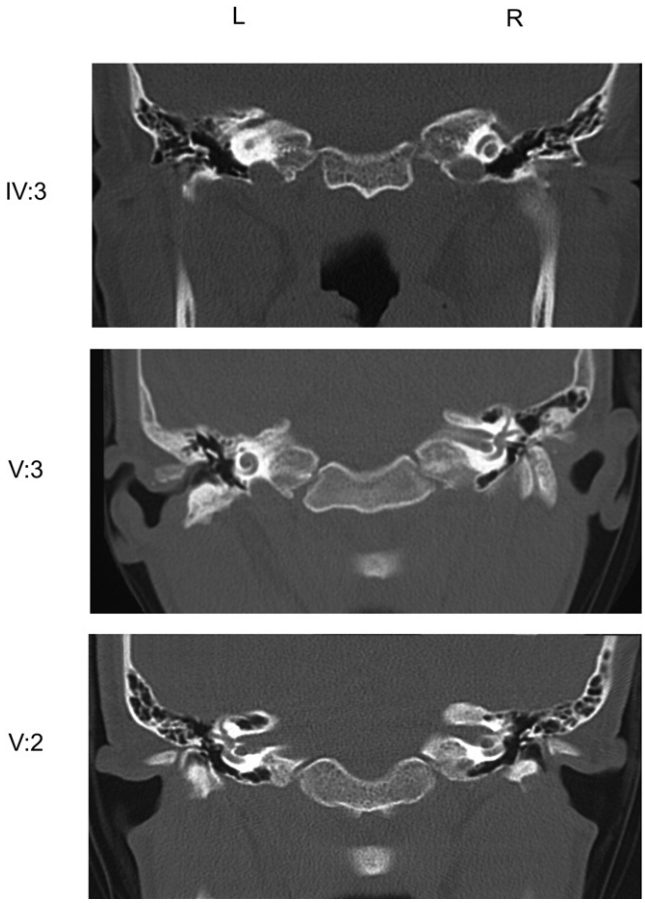

Figure 2. High-Resolution CT Imaging of Three Patients' Temporal Bones

These images (coronal views) present bilateral stenotic ear canals, an incomplete atretic plate, malformed ossicles, and a normal inner ear except in patient IV:3 on the left side.

sequence identity. The alignment and the Antennapedia homeodomain-DNA X-ray structure (pdb code 9ANT) was used for producing an ensemble of homology models with the program Modeler 8v2.[21]

Results

ENT-Examination Results

Three affected subjects V: 2, V: 3, and IV: 3 underwent detailed otorhinolaryngological assessments. The external examination of the ears revealed an abnormal shape of the auricle on both sides. Figure 1 shows a picture of the microtic ears of three affected members. Helix, tragus, and antitragus were seen in all patients. At otoscopy, the external auditory canal is short and severely narrowed bilaterally and almost stenotic in the three patients. Based on the abnormalities observed in this family, the disease was categorized as microtia grade II. A partial cleft palate was found in all three patients. Individual number V: 2 also had a paresis on the right side of the face.

High-Resolution CT Scan and MRI Results

A high-resolution CT scan of the ears was carried out for the patients V: 2, V: 3, and IV: 3. The results of high-resolution CT scanning confirmed that the external auditory canal was severely narrowed bilaterally in the cartilaginous part of the auditory canal and almost atretic in part of the bony portion in all patients. In individual V: 2, both tympanic membranes were visible but were hypoplastic because of an incomplete atretic plate. The mastoid air cells were normal in IV: 3 and V: 2, but in V: 3 the left ear developed poorly and the right ear showed a normal pneumatization. The middle ear cavities were normally aerated in all three individuals, but small in size in V: 2. In all three patients the malformed ossicular chain seemed fixated by an incomplete atretic plate. The inner-ear structures were normal in patients V: 2 and V: 3, but there were no inner-ear structures on the left side for IV: 3. Figure 2 shows a selection of these scans. The MRI of the auditory system in individual V: 3 was unremarkable for the inner ear and cerebellopontine angle, but an MRI confirmed the inner-ear agenesis on the left side of individual IV: 3 as seen on CT-images. The brain MRI of the patient with paresis was normal. On the basis of clinical examinations, hypoplasia of the 7th nerve on the right side was suspected.

Audiometric Results

An audiometric examination was performed for all participating members of family IR-SA-27. The onset of hearing

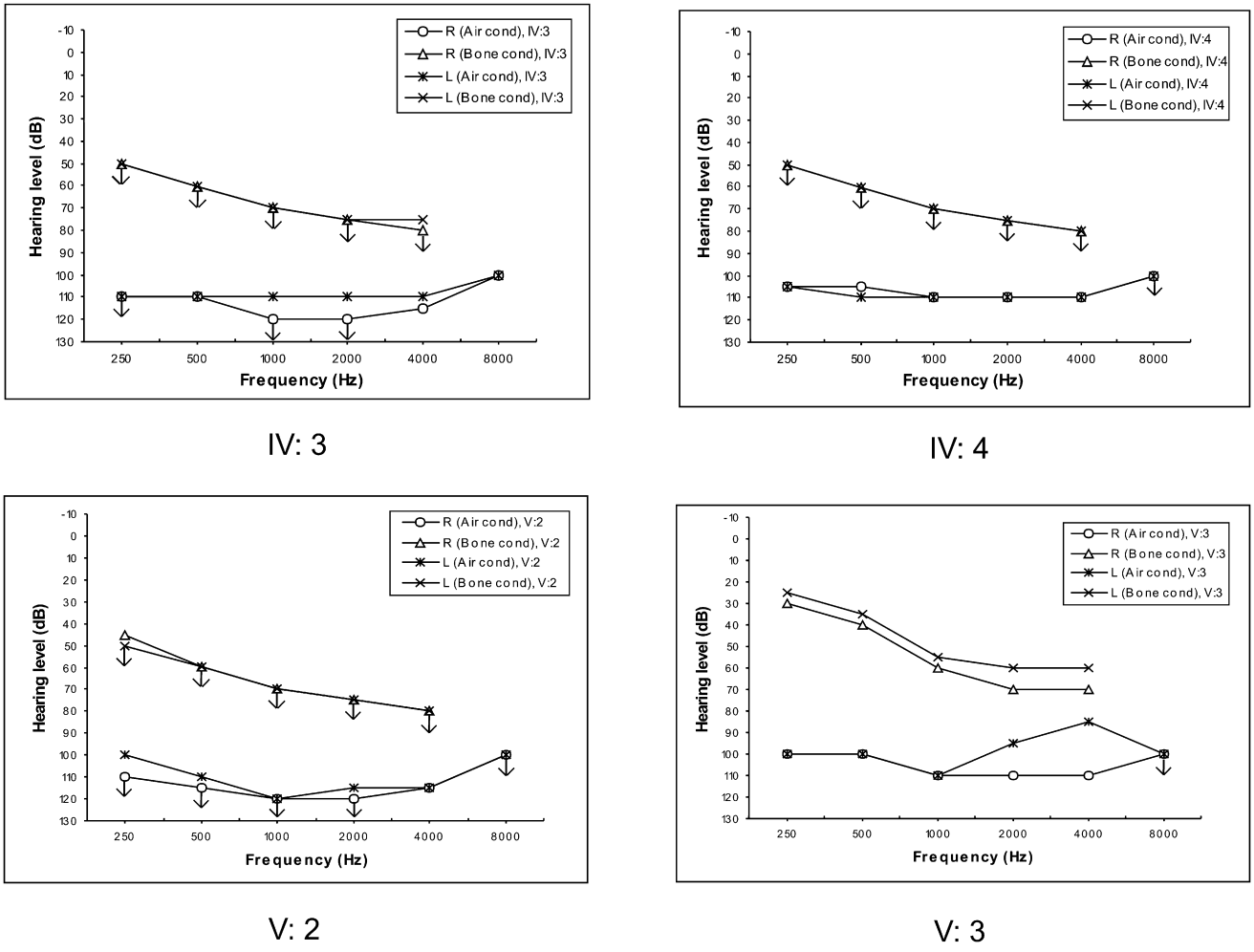

Figure 3. Pure-Tone Audiometry of Both Ears for All Four Affected Family Members
Audiometry was performed at frequencies of 250–8000 Hz for air conduction and 250–4000 Hz for bone conduction.

impairment in all four patients in this family was prelingual. All four affected family individuals showed bilateral symmetric severe to profound mixed hearing impairment affecting all frequencies and leading to a flat audiometric shape. Figure 3 shows the air- and bone-conduction pure-tone audiometric profile of both ears of all four affected family members. All heterozygous carriers in this family had normal hearing for their sex and age (data not shown).

Vestibular Test Results

VNG examination was normal in the individuals V: 2, V: 3, and IV: 3. Caloric stimulation (both air and water) could not be performed in the patients V: 3 and IV: 3, probably because of a narrow ear canal and insufficient stimulation, whereas in patient V: 2 the result was within normal limits. The other VNG test results were within normal limits in all three patients.

Additional Clinical Investigations

Three affected individuals of this family, IV: 3, V: 2, and V: 3, were investigated by means of additional general clinical tests such as blood biochemistry, urine analysis, hematology (CBC), electrocardiography and radiological X-ray examinations. The kidneys were also investigated bilaterally with ultrasonography. The results were all within normal range.

Linkage-Analysis Results

A genome-wide linkage analysis was carried out with 500 STRP markers for all ten available DNA samples of the family IR-SA-27. The results of the two-point LOD score analysis for the whole-genome linkage scan are presented in Figure S1. A maximum two-point LOD score of 2.87 and a maximum multi-point LOD score of 3.15 was obtained with markers D7S503, D7S629, and D7S2444 on chromosome 7p14.3-p15.3. For fine mapping, additional markers were selected from the deCode genetic map. Genotyping 15 additional markers and haplotype construction revealed an identical homozygous haplotype in all four affected individuals. A maximum multi-point LOD score of 4.17 was obtained with all markers across the interval. Two-point and multi-point LOD scores between the disease and chromosome 7 markers are presented in Table S2. The homozygous region was approximately 13.7 centi-Morgans (cM) and

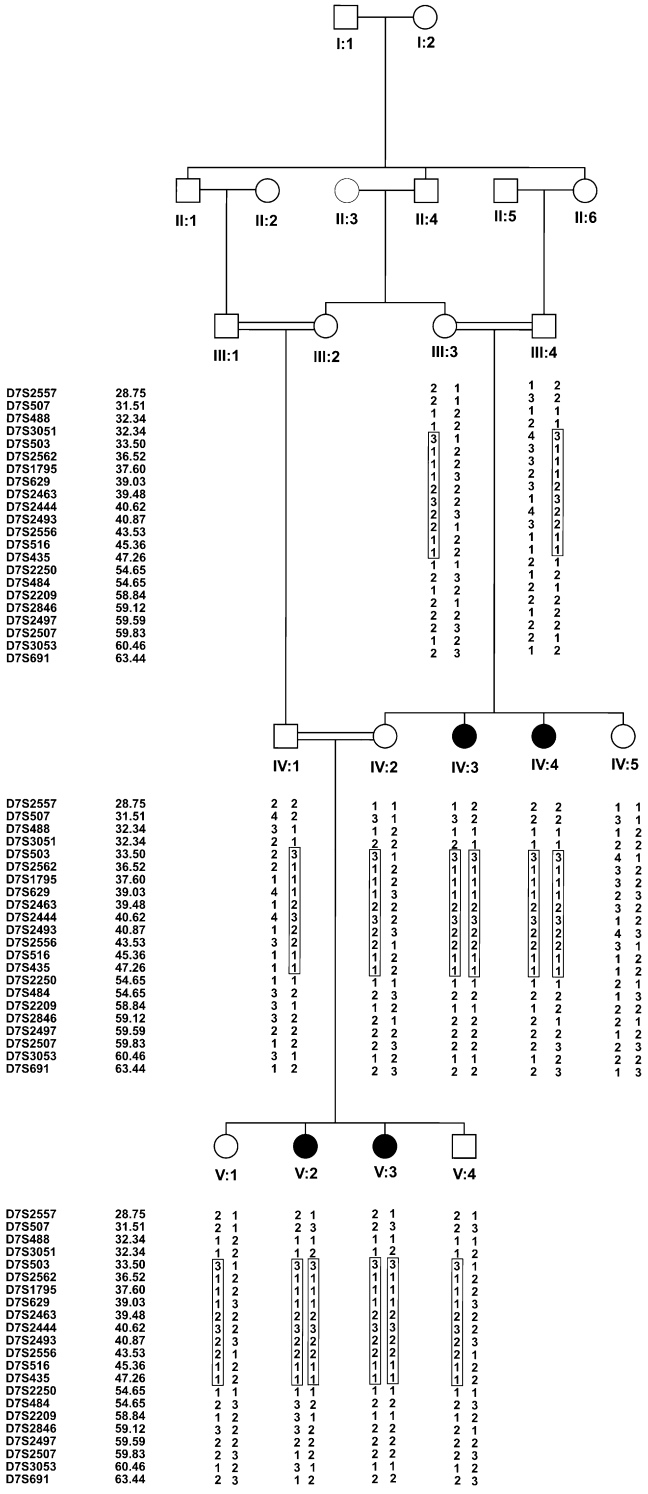

Figure 4. The Pedigree of the Iranian Consanguineous Family IR-SA-27 Segregating with Autosomal-Recessive Microtia

A double marriage line denotes consanguinity. Black symbols represent individuals with microtia, hearing impairment, and partial cleft palate. Clear symbols represent unaffected individuals. The boxed haplotype bars denote the disease–associated haplotype. The genetic-map distance in centi-Morgans (cM) is given in front of the marker names. Haplotypes for the analyzed STRPs are shown below each individual symbol.

was delimited by markers D7S503 (33.5 cM) and D7S435 (47.26 cM). The pedigree, haplotype, and a physical map of this locus interval are shown in Figure 4. A maximum multi-point LOD score of 4.17 was obtained from seven markers (D7S2562–D7S2556) in this region.

DNA-Sequencing Results

The genome-wide linkage analysis led to the localization of the responsible gene to a region of 9.9 Mb. This region includes more than 100 genes. Because the *HOXA* cluster (including 11 genes) falls in the homozygous region, mutation analysis of *HOXA1* and *HOXA2* was carried out. The DNA from one affected and one normal individual was used for sequencing. A missense variant c.558C > A was found in *HOXA2*. The variant cosegregated with the disease in the family and was heterozygous in the parents. It was not present in 231 Iranian and 109 Belgian control samples. Figure S2 shows the electropherograms of one normal, one heterozygous, and one homozygous family member for this mutation. The mutation causes an amino acid substitution at position 186 (p.Q186K) in the HOXA2 protein. The HOXA2 protein sequence was aligned with 100 different HOX proteins from different species. The Q at position 44 was conserved in all *Hox* genes analyzed, including HoxA, B, C and D from several mammals and nonmammals. The ConSeq server was used for checking the conservation of the amino acid position 186. The ConSeq score for the residue 186 was 9, indicating very high evolutionary conservation. Figure 5 shows a selected part of this alignment.

Model-Building Results

We built a model for predicting the effect of this mutation on the structure and DNA-binding activity of the homeodomain by using the program Modeler 8v2. As expected, the overall structure of the wild-type HOXA2 homeodomain-DNA model is very similar to the Antennapedia homeodomain complex. In both cases, the majority of protein-DNA contacts are mediated by the N-terminal arm and the recognition helix (Figure 6A). The mutated amino acid is located at position 186 of the protein, which is the position 44 of homeodomain. Q44 is found in the recognition helix and contributes to binding through favorable packing against residues in the N-terminal arm and a hydrogen bond to the phosphate group of a central adenine in the TAAT DNA-binding motif. Y8 from the N-terminal arm also hydrogen bonds to this phosphate group (Figure 6B). In the mutant Q44K HOXA2 homeodomain models, the position of the lysine side chain is consistently away from the phosphate group and thereby leads to loss of the hydrogen bond (Figure 6C). Based on a previous study of charge and stability of homeodomains,[22] it is likely that the mutant protein will be less stable than the wild-type as a result of charge repulsion in an already highly basic molecule. These results indicate that, from a structural perspective, it is highly likely that the HOXA2 homeodomain binding properties will change as a result of the Q to K mutation.

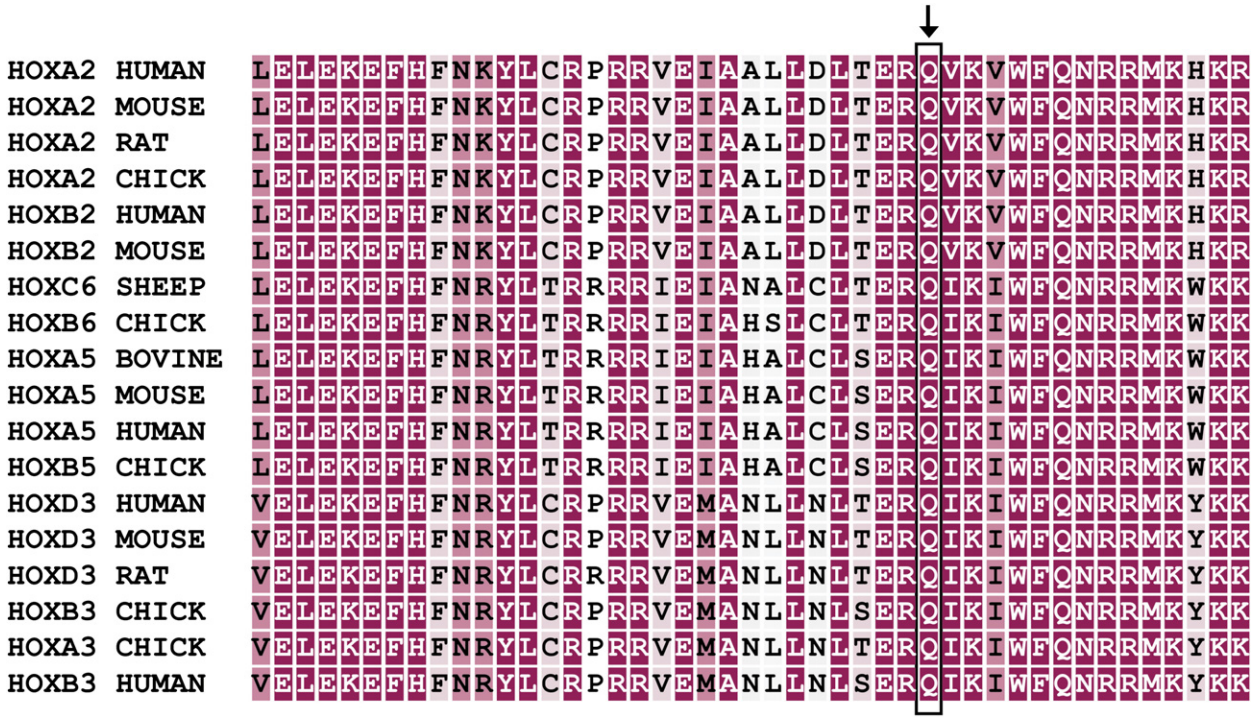

Figure 5. ConSeq Conservation Analysis of the Amino Acid Q44 in Homeodomain of the Human HOXA2 Protein
This analysis is based on the alignment of 100 full-length members of different *HOX* gene clusters in different species. Colors indicate the degree of conservation of each residue. In the figure, the alignment of only 18 proteins is shown.

Discussion

Homeobox genes encode transcription factors that typically switch on cascades of other genes in embryonic development.[23] They are a conserved set of developmental regulatory genes, all sharing a 180 bp segment of DNA. *Hox* genes are a subset of homeobox genes of which there are four cluster groups (A–D) in vertebrates.[24] The number of *Hox* genes is four to 48 per genome, depending on the animal.[25] In humans there are 39 homeobox genes of the HOX family at four loci, HOXA, HOXB, HOXC, and HOXD on chromosomes 7, 17, 12, and 2, respectively.[26]

All *Hox* genes encode proteins that share a 60 amino acid domain called the homeodomain. This structural motif is found in many different transcription regulators for a wide range of genes and plays developmentally

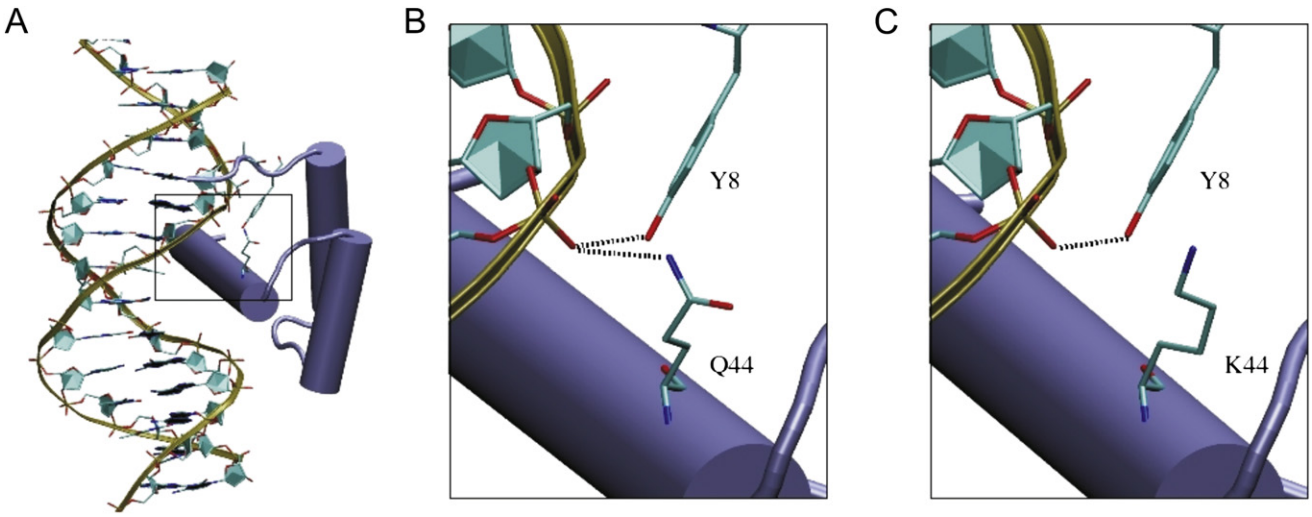

Figure 6. Representative Homology Models of the HOXA2 Homeodomain Bound to DNA
Overall schematic diagram of the protein-DNA complex (A) and close-up views of the wild-type (B) and Q44K (C) homeodomains. Hydrogen bonds are indicated by dashed lines.

important roles in cell differentiation in a variety of organisms.[27] Mutations in homeobox genes result in the transformation of different parts of the body during development.[28–30] A homeodomain is a helix-turn-helix motif consisting of three alpha-helices and an N-terminal arm. Site-specific DNA binding is achieved by interaction of the third helix with the major DNA groove. The N-terminal arm residues normally mediate contacts with the minor groove of DNA.[31,32] Different pathogenic changes in the sequence of a homeodomain can affect stability and/or DNA-binding activity.[32,33]

HoxA cluster genes are fundamental players in the building of the sensorimotor circuitry in vertebrates.[34] *HoxA2,* a member of the *HOXA* cluster, encodes a protein with a molecular weight of 41kD and is important in the regulation of development and morphogenesis in different eukaryotes.[35,36]

Knockout experiments have demonstrated that the *Hox* genes (including the *HoxA* genes) are involved in patterning the antero-posterior axis of the embryo of almost all metazoans. *HoxA2* is most probably involved in patterning and morphogenesis of the neural-crest-derived mesenchyme.[37–39] It has an important role in hindbrain segmentation.[36] *HoxA2* is expressed during development of the mouse neural tube and has an anterior limit corresponding to the boundary between rhombomeres 1 and 2. Rhombomeres are embryonic territories arising from the transient segmentation of the hindbrain.[36–39] In *HoxA2*$^{-/-}$ mice, the neural crest cell-derived structures from the second branchial arch are transformed into structures of the first branchial arch, resulting in the transformation of some elements of the jaw, as well as of occipital and middle ear bones.[36,39]

HoxA2 is the only *Hox* gene expressed in the second rhombomere.[40,41] It is a key transcription factor during development of the second branchial arch, which makes a major contribution in development of the external ear.[42] The mechanism by which HoxA2 regulates the morphology of the second branchial arch derivatives is unclear, like most of the developmental processes controlled by Hox proteins. However, the contribution of the second branchial arch to the development of the middle ear is clear from the study of the *HoxA2* knockout mouse.[36,39,42] HoxA2 appears not only to affect the patterning of the tympanic ring and gonial bone but also to synergize with HoxA1 in controlling the growth of these structures.[43]

The phenotype of *HoxA2* knockout mice includes lack of pinna and processus brevis and duplication of the malleus and the squamous bones. Other mesenchymal structures partly derived from the second arch were also affected; these included parts of the cartilaginous otic capsule.[36,39] From the study of these mice, we know that the HoxA2 protein is important for the development of the auditory system, mainly the outer and middle ear. The embryological origin of the inner ear is different than that of the middle ear and outer ear, which share a common origin. The inner ear is derived from an epidermal otic placode at the level of the hindbrain, whereas the middle ear and outer ear originate from the mesenchyme at the first and second pharyngeal or branchial arches.[44,45]

The formation of many craniofacial tissues is influenced by *Hox* genes. *Hoxa2* is also a key gene for the facial somatosensory map.[46,47] A significant percentage of microtic patients also present deficient facial components that originate from the same embryological structures.[46,48] All affected members of the family IR-SA-27 also show a partial cleft palate. A facial motor problem is an additional problem found in only one affected member of the family.

The *HoxA2* knockout mice are born with a bilateral cleft of the secondary palate, and they die within 24 hr of birth.[36,39,49] *HoxA2* is expressed in the mesenchyme and epithelial cells of the palate at E12 in the normal mice, but by the E15 stage of development, *HoxA2* is downregulated in the palate and expression is localized in the nasal and oral epithelia.[50] *HoxA2* mRNA and protein expression were significantly decreased in an animal model of phenytoin-induced cleft palate.[50] The phenotype of partial cleft palate in family IR-SA-27 is a strong indication of the putative role of this gene in palate development.

In microtic patients, there is often a correlation between the level of malformation of the outer and middle ear, which is not surprising in view of their common origin. An external ear with better development usually shows a better developed middle ear.[51] In the family IR-SA-27, all affected individuals share the same phenotype for the external and middle ear. Surprisingly, individual IV: 3 shows severe abnormalities of the left-sided inner ear. This is a remarkable point because all the previous studies on *HoxA2* knockout mice have shown severe outer- and middle-ear anomalies, but a malformation of the otic capsule is the only determined defect in the inner ear.

Although most of the microtic patients have a normal inner ear,[17,52] the combination of microtia with inner-ear anomalies has also been reported.[17] A Japanese family was reported with inner-ear semicircular canal malformation and external- and middle-ear abnormalities.[53] This condition supports a genetic basis for the combination of abnormalities in the semicircular canal, external ear, and middle ear. In a study in Belgium, 8% (13/166) of microtic patients presented inner-ear abnormalities that were visible on CT or MRI or were demonstrated by some perceptive loss during tonal audiometry (T.S., unpublished data). Based on the audiometric profile, 8% of microtic patients in Finland have sensorineural hearing loss and present with inner-ear abnormalities.[54] A combination of microtia type I and complete absence of the inner ear has also been reported.[17]

In most microtia patients, the affected microtic ear usually has conductive hearing loss, and air-conduction hearing is typically reduced by 40–67 dB in all four grades of microtia.[54,55] However, bone-conduction hearing thresholds are not affected in most microtia patients, indicating that the hearing impairment is only conductive and that the inner ear is functionally intact. In family IR-SA-27, however, the hearing impairment is not only conductive

but also shows a sensorineural component. Because of this fact, the air-conduction Fletcher index in our patients is higher than in most other microtia patients. These findings implicate the inner ear in the pathology of this family. However, imaging only showed inner-ear abnormalities in one out of eight ears. Imaging abnormalities of the inner ear are detected in almost 30% of sensorineural-hearing-loss patients.[56,57]

In the mouse, there are several homeobox gene mutations that are associated with microtia. A dominant mutation of the murine *Hox-2.2* gene (homolog for *HOXB6* [MIM *142961] in humans) has been shown to cause open eyes at birth, cleft palate, and microtia.[58] The homeobox gene *Emx2* underlies defects in the middle ear and inner ear in the deaf mouse mutant pardon (*Pdo*).[59] Mice that are homozygous mutant for the *HoxA1* gene die at birth from anoxia and exhibit marked defects in the inner ear.[43,60–62] In humans, a homozygous mutation in *HOXA1* disrupts the inner ear and the outer ear to various degrees and also results in facial and brainstem abnormalities.[14] Therefore, *HOXB6, EMX2* (MIM *600035), and *HOXA1* also might be functional candidate genes for microtia in humans.

The missense mutation found in the microtia family in this study affects position 44 of the homeodomain. Position 44 is a surface-exposed residue found in the recognition helix and is very well conserved in different homeodomains. We aligned the human HOXA2 protein with the Antennapedia homeodomain (Ant-HD) (58% sequence identity) and used the Ant-HD/DNA X-ray structure (pdb code 9ANT.pdb) to produce a homology model by using the program Modeler. We feel confident in using the model because the homeodomain fold is a common and stable fold and always uses the same binding surface to specifically bind DNA. We see that the Q44K mutation destroys a hydrogen bond between the homeodomain and the DNA, and loss of this bond would reduce the binding affinity. The mutation will also cause electrostatic repulsion with its neighboring DNA-binding residue, Arginine 43. In fact, the addition of another positive charge to an already highly basic protein (net +8) will cause an overall destabilization of the homeodomain, and this destabilization will also impact the binding properties. Taken together, we hypothesize that the Q44K mutant removes a hydrogen bond to the DNA and introduces electrostatic repulsion, which has a large impact on protein function.

We have searched the genetic literature and databases, such as OMIM, POSSUM, and London dysmorphology medical database (LDDB)[63] for patients or families with the same symptoms (microtia, mixed hearing loss, inner ear abnormality and cleft palate) as the current family. We have not been successful in this regard because these four symptoms, if present, are always seen in combination with other abnormalities. We conclude that the phenotypic findings described in this family represent a distinct autosomal-recessive disease. Although we feel that the evidence for the involvement of a mutation in *HOXA2* in auditory-system malformations is very strong, formal proof needs to come from the identification of additional patients with mutations or from future functional assays on the DNA-binding activity of the mutant protein.

Supplemental Data

Two figures and two tables are available online at http://www.ajhg.org/.

Acknowledgments

We would like to thank the family members of IR-SA-27 for their participation and cooperation. We are grateful to Lut Van Laer, Jan-Jaap Hendrickx, Paul Van De Heyning, and Jenneke Van Ende for their useful comments and remarks on this project. We also thank Saeid Mahmoudian from the Iran Cochlear Implant Center for his great efforts in preparing the vestibular tests and Jeroen Huyghe for his help with the linkage analysis. This work was supported by the European Commission (FP6 Integrated project EuroHear LSHG-CT-20054-512063), the Flemish FWO (grant G.0138.07), and the National Institute for Genetic Engineering and Biotechnology (grant number 164), Tehran, Iran.

Received: January 17, 2008
Revised: February 12, 2008
Accepted: February 28, 2008
Published online: April 3, 2008

Web Resources

The URLs for data presented herein are as follows:

Hereditary hearing loss homepage, http://webh01.ua.ac.be/hhh/
Ensembl, http://www.ensembl.org/Homo_sapiens/geneview/
GenBank, http://www.ncbi.nlm.nih.gov/Genbank/
ConSeq server, http://conseq.bioinfo.tau.ac.il/ for alignment of different homeodomains from different species
easyLINKAGE plus v4.01beta software, http://sourceforge.net/projects/easylinkage/, for two-point and multi-point parametric linkage analysis
Online Mendelian Inheritance in Man (OMIM), http://www.ncbi.nlm.nih.gov/omim/

Accession Numbers

Numbering of nucleotides of the *HOXA2* gene is according to the Genbank sequence accession number NT_007819.

References

1. Sanchez, O., Mendez, J.R., Gomez, E., and Guerra, D. (1997). Invest. Clin. *38*, 203–217.
2. Mastroiacovo, P., Corchia, C., Botto, L.D., Lanni, R., Zampino, G., and Fusco, D. (1995). Epidemiology and genetics of microtia-anotia: A registry based study on over one million births. J. Med. Genet. *32*, 453–457.
3. Harris, J., Kallen, B., and Robert, E. (1996). The epidemiology of anotia and microtia. J. Med. Genet. *33*, 809–813.
4. Okajima, H., Takeichi, Y., Umeda, K., and Baba, S. (1996). Clinical analysis of 592 patients with microtia. Acta Otolaryngol. Suppl. *525*, 18–24.

5. Shaw, G.M., Carmichael, S.L., Kaidarova, Z., and Harris, J.A. (2004). Epidemiologic characteristics of anotia and microtia in California, 1989–1997. Birth Defects Res. A Clin. Mol. Teratol. *70*, 472–475.
6. Meurman, Y. (1957). Congenital microtia and meatal atresia; Observations and aspects of treatment. AMA Arch. Otolaryngol. *66*, 443–463.
7. Wang, R.Y., Earl, D.L., Ruder, R.O., and Graham, J.M. Jr. (2001). Syndromic ear anomalies and renal ultrasounds. Pediatrics *108*, E32.
8. Forrester, M.B., and Merz, R.D. (2005). Descriptive epidemiology of anotia and microtia, Hawaii, 1986–2002. Congenit. Anom. (Kyoto) *45*, 119–124.
9. Castori, M., Brancati, F., Rinaldi, R., Adami, L., Mingarelli, R., Grammatico, P., and Dallapiccola, B. (2006). Antenatal presentation of the oculo-auriculo-vertebral spectrum (OAVS). Am. J. Med. Genet. A. *140*, 1573–1579.
10. Llano-Rivas, I., Gonzalez-del Angel, A., del Castillo, V., Reyes, R., and Carnevale, A. (1999). Microtia: A clinical and genetic study at the National Institute of Pediatrics in Mexico City. Arch. Med. Res. *30*, 120–124.
11. Moore, J.K., Guan, Y.L., and Shi, S.R. (1998). MAP2 expression in developing dendrites of human brainstem auditory neurons. J. Chem. Neuroanat. *16*, 1–15.
12. Lynberg, M.C., Khoury, M.J., Lammer, E.J., Waller, K.O., Cordero, J.F., and Erickson, J.D. (1990). Sensitivity, specificity, and positive predictive value of multiple malformations in isotretinoin embryopathy surveillance. Teratology *42*, 513–519.
13. Tasse, C., Bohringer, S., Fischer, S., Ludecke, H.J., Albrecht, B., Horn, D., Janecke, A., Kling, R., Konig, R., Lorenz, B., et al. (2005). Oculo-auriculo-vertebral spectrum (OAVS): Clinical evaluation and severity scoring of 53 patients and proposal for a new classification. Eur. J. Med. Genet. *48*, 397–411.
14. Tischfield, M.A., Bosley, T.M., Salih, M.A., Alorainy, I.A., Sener, E.C., Nester, M.J., Oystreck, D.T., Chan, W.M., Andrews, C., Erickson, R.P., et al. (2005). Homozygous HOXA1 mutations disrupt human brainstem, inner ear, cardiovascular and cognitive development. Nat. Genet. *37*, 1035–1037.
15. Marszalek, B., Wojcicki, P., Kobus, K., and Trzeciak, W.H. (2002). Clinical features, treatment and genetic background of Treacher Collins syndrome. J. Appl. Genet. *43*, 223–233.
16. Stevenson, D.A., Bleyl, S.B., Maxwell, T., Brothman, A.R., and South, S.T. (2007). Mandibulofacial dysostosis in a patient with a de novo 2;17 translocation that disrupts the HOXD gene cluster. Am. J. Med. Genet. A. *143*, 1053–1059.
17. Tekin, M., Hismi, B.O., Fitoz, S., Ozdag, H., Cengiz, F.B., Sirmaci, A., Aslan, I., Inceoglu, B., Yuksel-Konuk, E.B., Yilmaz, S.T., et al. (2007). Homozygous mutations in fibroblast growth factor 3 are associated with a new form of syndromic deafness characterized by inner ear agenesis, microtia, and microdontia. Am. J. Hum. Genet. *80*, 338–344.
18. Stoll, C., Medeiros, P., Pecheur, H., and Schnebelen, A. (1997). De novo trisomy 22 due to an extra 22Q-chromosome. Ann. Genet. *40*, 217–221.
19. Grimberg, J., Nawoschik, S., Belluscio, L., McKee, R., Turck, A., and Eisenberg, A. (1989). A simple and efficient non-organic procedure for the isolation of genomic DNA from blood. Nucleic Acids Res. *17*, 8390.
20. Berezin, C., Glaser, F., Rosenberg, J., Paz, I., Pupko, T., Fariselli, P., Casadio, R., and Ben-Tal, N. (2004). ConSeq: the identification of functionally and structurally important residues in protein sequences. Bioinformatics *20*, 1322–1324.
21. Sali, A., and Blundell, T.L. (1993). Comparative protein modelling by satisfaction of spatial restraints. J. Mol. Biol. *234*, 779–815.
22. Stollar, E.J., Mayor, U., Lovell, S.C., Federici, L., Freund, S.M., Fersht, A.R., and Luisi, B.F. (2003). Crystal structures of engrailed homeodomain mutants: Implications for stability and dynamics. J. Biol. Chem. *278*, 43699–43708.
23. Mark, M., Rijli, F.M., and Chambon, P. (1997). Homeobox genes in embryogenesis and pathogenesis. Pediatr. Res. *42*, 421–429.
24. Scott, M.P. (1992). Vertebrate homeobox gene nomenclature. Cell *71*, 551–553.
25. Lemons, D., and McGinnis, W. (2006). Genomic evolution of Hox gene clusters. Science *313*, 1918–1922.
26. Faiella, A., Zortea, M., Barbaria, E., Albani, F., Capra, V., Cama, A., and Boncinelli, E. (1998). A genetic polymorphism in the human HOXB1 homeobox gene implying a 9bp tandem repeat in the amino-terminal coding region. Mutations in brief no. 200. Online. Hum. Mutat. *12*, 363.
27. Burglin, T.R. (1997). Analysis of TALE superclass homeobox genes (MEIS, PBC, KNOX, Iroquois, TGIF) reveals a novel domain conserved between plants and animals. Nucleic Acids Res. *25*, 4173–4180.
28. Gehring, W.J., Affolter, M., and Burglin, T. (1994). Homeodomain proteins. Annu. Rev. Biochem. *63*, 487–526.
29. Garcia-Fernandez, J. (2005). The genesis and evolution of homeobox gene clusters. Nat. Rev. Genet. *6*, 881–892.
30. Kissinger, C.R., Liu, B.S., Martin-Blanco, E., Kornberg, T.B., and Pabo, C.O. (1990). Crystal structure of an engrailed homeodomain-DNA complex at 2.8 A resolution: A framework for understanding homeodomain-DNA interactions. Cell *63*, 579–590.
31. Phelan, M.L., Sadoul, R., and Featherstone, M.S. (1994). Functional differences between HOX proteins conferred by two residues in the homeodomain N-terminal arm. Mol. Cell. Biol. *14*, 5066–5075.
32. Gehring, W.J., Qian, Y.Q., Billeter, M., Furukubo-Tokunaga, K., Schier, A.F., Resendez-Perez, D., Affolter, M., Otting, G., and Wuthrich, K. (1994). Homeodomain-DNA recognition. Cell *78*, 211–223.
33. Kappen, C., Schughart, K., and Ruddle, F.H. (1993). Early evolutionary origin of major homeodomain sequence classes. Genomics *18*, 54–70.
34. Oury, F., Murakami, Y., Renaud, J.S., Pasqualetti, M., Charnay, P., Ren, S.Y., and Rijli, F.M. (2006). Hoxa2- and rhombomere-dependent development of the mouse facial somatosensory map. Science *313*, 1408–1413.
35. Bobola, N., Carapuco, M., Ohnemus, S., Kanzler, B., Leibbrandt, A., Neubuser, A., Drouin, J., and Mallo, M. (2003). Mesenchymal patterning by Hoxa2 requires blocking Fgf-dependent activation of Ptx1. Development *130*, 3403–3414.
36. Gendron-Maguire, M., Mallo, M., Zhang, M., and Gridley, T. (1993). Hoxa-2 mutant mice exhibit homeotic transformation of skeletal elements derived from cranial neural crest. Cell *75*, 1317–1331.
37. Davenne, M., Maconochie, M.K., Neun, R., Pattyn, A., Chambon, P., Krumlauf, R., and Rijli, F.M. (1999). Hoxa2 and Hoxb2 control dorsoventral patterns of neuronal development in the rostral hindbrain. Neuron *22*, 677–691.
38. Gavalas, A., Davenne, M., Lumsden, A., Chambon, P., and Rijli, F.M. (1997). Role of Hoxa-2 in axon pathfinding and rostral hindbrain patterning. Development *124*, 3693–3702.

39. Rijli, F.M., Mark, M., Lakkaraju, S., Dierich, A., Dolle, P., and Chambon, P. (1993). A homeotic transformation is generated in the rostral branchial region of the head by disruption of Hoxa-2, which acts as a selector gene. Cell *75*, 1333–1349.
40. Tan, D.P., Ferrante, J., Nazarali, A., Shao, X., Kozak, C.A., Guo, V., and Nirenberg, M. (1992). Murine Hox-1.11 homeobox gene structure and expression. Proc. Natl. Acad. Sci. USA *89*, 6280–6284.
41. Lampe, X., Picard, J.J., and Rezsohazy, R. (2004). The Hoxa2 enhancer 2 contains a critical Hoxa2 responsive regulatory element. Biochem. Biophys. Res. Commun. *316*, 898–902.
42. O'Gorman, S. (2005). Second branchial arch lineages of the middle ear of wild-type and Hoxa2 mutant mice. Dev. Dyn. *234*, 124–131.
43. Barrow, J.R., Stadler, H.S., and Capecchi, M.R. (2000). Roles of Hoxa1 and Hoxa2 in patterning the early hindbrain of the mouse. Development *127*, 933–944.
44. Mallo, M. (2001). Formation of the middle ear: recent progress on the developmental and molecular mechanisms. Dev. Biol. *231*, 410–419.
45. Nishikori, T., Hatta, T., Kawauchi, H., and Otani, H. (1999). Apoptosis during inner ear development in human and mouse embryos: An analysis by computer-assisted three-dimensional reconstruction. Anat. Embryol. (Berl.) *200*, 19–26.
46. Couly, G., Grapin-Botton, A., Coltey, P., Ruhin, B., and Le Douarin, N.M. (1998). Determination of the identity of the derivatives of the cephalic neural crest: Incompatibility between Hox gene expression and lower jaw development. Development *125*, 3445–3459.
47. Oury, F., and Rijli, F.M. (2007). Med. Sci. (Paris) *23*, 247–249.
48. Takegoshi, H., Kaga, K., and Chihara, Y. (2005). Facial canal anatomy in patients with mandibulofacial dysostosis: Comparison with respect to the severities of microtia and middle ear deformity. Otol. Neurotol. *26*, 803–808.
49. Mallo, M., and Gridley, T. (1996). Development of the mammalian ear: Coordinate regulation of formation of the tympanic ring and the external acoustic meatus. Development *122*, 173–179.
50. Nazarali, A., Puthucode, R., Leung, V., Wolf, L., Hao, Z., and Yeung, J. (2000). Temporal and spatial expression of Hoxa-2 during murine palatogenesis. Cell. Mol. Neurobiol. *20*, 269–290.
51. Kountakis, S.E., Helidonis, E., and Jahrsdoerfer, R.A. (1995). Microtia grade as an indicator of middle ear development in aural atresia. Arch. Otolaryngol. Head Neck Surg. *121*, 885–886.
52. Williamson, I. (2007). Review: Children <2 years of age with bilateral acute otitis media and children with otorrhoea benefit most from antibiotics. Arch. Dis. Child Educ. Pract. Ed. *92*, ep159.
53. Kimitsuki, T., Inamitsu, M., Komune, S., and Komiyama, S. (1999). Congenital malformation of the inner ear associated with recurrent meningitis. Eur. Arch. Otorhinolaryngol. *256* (*Suppl 1*), S11–S14.
54. Suutarla, S., Rautio, J., Ritvanen, A., Ala-Mello, S., Jero, J., and Klockars, T. (2007). Microtia in Finland: Comparison of characteristics in different populations. Int. J. Pediatr. Otorhinolaryngol. *71*, 1211–1217.
55. Ishimoto, S., Ito, K., Karino, S., Takegoshi, H., Kaga, K., and Yamasoba, T. (2007). Hearing levels in patients with microtia: Correlation with temporal bone malformation. Laryngoscope *117*, 461–465.
56. Bamiou, D.E., Phelps, P., and Sirimanna, T. (2000). Temporal bone computed tomography findings in bilateral sensorineural hearing loss. Arch. Dis. Child. *82*, 257–260.
57. Mafong, D.D., Shin, E.J., and Lalwani, A.K. (2002). Use of laboratory evaluation and radiologic imaging in the diagnostic evaluation of children with sensorineural hearing loss. Laryngoscope *112*, 1–7.
58. Kaur, S., Singh, G., Stock, J.L., Schreiner, C.M., Kier, A.B., Yager, K.L., Mucenski, M.L., Scott, W.J. Jr., and Potter, S.S. (1992). Dominant mutation of the murine Hox-2.2 gene results in developmental abnormalities. J. Exp. Zool. *264*, 323–336.
59. Rhodes, C.R., Parkinson, N., Tsai, H., Brooker, D., Mansell, S., Spurr, N., Hunter, A.J., Steel, K.P., and Brown, S.D. (2003). The homeobox gene Emx2 underlies middle ear and inner ear defects in the deaf mouse mutant pardon. J. Neurocytol. *32*, 1143–1154.
60. Mark, M., Lufkin, T., Vonesch, J.L., Ruberte, E., Olivo, J.C., Dolle, P., Gorry, P., Lumsden, A., and Chambon, P. (1993). Two rhombomeres are altered in Hoxa-1 mutant mice. Development *119*, 319–338.
61. Lufkin, T., Dierich, A., LeMeur, M., Mark, M., and Chambon, P. (1991). Disruption of the Hox-1.6 homeobox gene results in defects in a region corresponding to its rostral domain of expression. Cell *66*, 1105–1119.
62. Chisaka, O., Musci, T.S., and Capecchi, M.R. (1992). Developmental defects of the ear, cranial nerves and hindbrain resulting from targeted disruption of the mouse homeobox gene Hox-1.6. Nature *355*, 516–520.
63. Pelz, J., Arendt, V., and Kunze, J. (1996). Computer assisted diagnosis of malformation syndromes: An evaluation of three databases (LDDB, POSSUM, and SYNDROC). Am. J. Med. Genet. *63*, 257–267.